Infrared reflectance studies on a Fe_3O_4 film deposited on a MgO substrate: Observation of the substrate longitudinal optic phonon resonance peak in the film geometry

J. S. Ahn,* H. S. Choi, and T. W. Noh†
Department of Physics and Condensed Matter Research Institute, Seoul National University, Seoul 151-742, Republic of Korea
(Received 3 October 1995; revised manuscript received 14 December 1995)

Infrared reflectance spectra were measured on a Fe_3O_4 film deposited on a bulk MgO substrate. For an obliquely incoming light with TM polarization, the reflectance spectra showed a peak structure near a longitudinal optic (LO) phonon frequency of MgO. For TE polarization, such a resonant structure was not observed. This phenomenon is quite different from the ''Berreman effect'' [D. W. Berreman, Phys. Rev. **130**, 2193 (1963)], where an absorption process related to a LO phonon of the film occurs instead of that of the substrate. For our film geometry, the electric field component normal to the film induces charge oscillations and a coupling between the charge carriers in the film and the LO phonon of MgO results in the resonance phenomenon. The resonance peak occurs at a frequency where the substrate dielectric constant becomes the same as $\sin^2\theta_0$, where θ_0 is the incident angle. This newly observed phenomenon might be useful to investigate a LO phonon of a solid, where other methods are difficult to be applied.

I. INTRODUCTION

Responses due to transverse optic (TO) and longitudinal optic (LO) phonons of a solid are related to poles and zeros of its dielectric constant, $\tilde{\epsilon}(\omega)$, respectively.[1,2] For a bulk sample with an isotropic $\tilde{\epsilon}(\omega)$, it has been shown that an electromagnetic wave, which is transverse, cannot interact with a LO phonon inside the infinite medium.[3,4] When the light enters a thin film with normal incidence, its transmission and reflectance spectra exhibit characteristic structures at the TO phonon frequency, ω_{TO}, but no characteristic structure appears at the LO phonon frequency, ω_{LO}. However, Berreman showed that characteristic structures would appear at ω_{LO} when a TM-polarized light entered a film with an oblique angle.[5] In this polarization, the electric field has a component normal to the surface of the film. The surface charges produced by this electric field component make a strong absorption at ω_{LO}, providing dip structures in transmission and reflectance spectra of the film. This phenomenon, called the ''Berreman effect,'' has been widely used to determine features of the LO modes in metal/insulator superlattices and insulating thin films.[5–11]

In this paper we report off-normal infrared reflectance spectra of a Fe_3O_4 film grown on a MgO substrate by pulsed laser deposition. These spectra show an interesting new phenomenon: reflectance spectra in TM polarization show a peak structure near ω_{LO} of MgO, $\omega_{\mathrm{LO}}^{\mathrm{MgO}}$. Note that this phenomenon is quite different from the Berreman effect, where the LO phonon of the film is involved in absorption process. The appearance of the resonance peak near ω_{LO} of the substrate can be understood qualitatively in a simple model based on a coupling between the carriers in the Fe_3O_4 film and the LO phonons of MgO.

The organization of this paper is as follows. In Sec. II, the experimental techniques including growth and infrared measurements of the Fe_3O_4 film on MgO are described. Also, the infrared spectra of Fe_3O_4/MgO are shown under various experimental conditions, such as various polarizations and incident angles of light. In Sec. III, a model which is used in theoretical predictions is described. Computer simulations show that the appearance of the substrate LO phonon resonance (LOPR) peak is contained in the Fresnel formula, just like the Berreman effect. However, since the Fresnel formula is quite complicated and nonlinear, a simple picture is desirable to get a clear understanding on why it happens. In Sec. IV, discussions based on computer simulations are given. A longitudinal response inside the metallic film, induced by the normal component of the electromagnetic wave, seems to be coupled with the MgO LO phonon and provides the resonance peak. The angular dependence of the peak frequency is also explained. In Sec. V, our results are summarized.

II. EXPERIMENTS

An epitaxial Fe_3O_4 film was grown on a MgO(001) substrate by pulsed laser deposition. Third harmonics (wavelength: 355 nm) of a *Q*-switched Nd:YAG laser was used. The laser beam was pulsed at a rate of 10 Hz and focused with a quartz lens onto a polycrystalline Fe_3O_4 target. During the deposition, the single-crystal MgO(001) substrate was maintained at a temperature of 350 °C and a base pressure of 3×10^{-5} Torr. The thickness of the film was estimated to be about 3000 Å. Details about growth and physical properties of the Fe_3O_4 film were published elsewhere.[12]

Infrared reflectance spectra of the Fe_3O_4 thin film were measured using a Fourier transform infrared spectrophotometer in a frequency region of 70–4000 cm^{-1}. The incident angle, θ_0, was able to be changed from 10° to 80° using a variable angle reflectance accessory. To study polarization dependence, the incident light was polarized with a wire grid polarizer on a KRS-5 substrate. Due to the absorption of KRS-5, the polarization studies were limited to a frequency region above 340 cm^{-1}.

A measured infrared reflectance spectrum of the Fe_3O_4 thin film is shown in Fig. 1(a) as solid circles, where an unpolarized light was used and θ_0 was fixed at 30°. Since

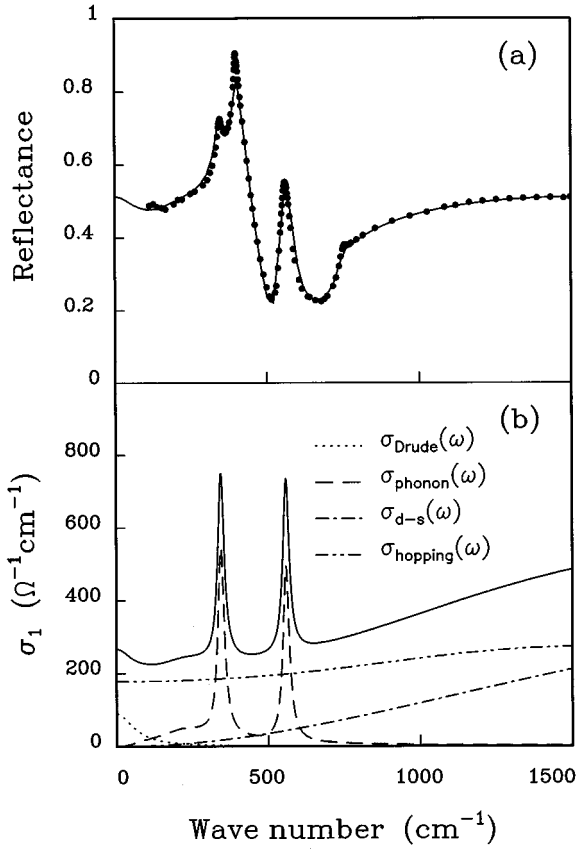

FIG. 1. (a) IR reflectance spectra of a Fe_3O_4 thin film grown on a MgO substrate, where unpolarized light enters with incident angle of 30°. Measured data and calculated ones are shown as solid circles and a solid line, respectively. (b) The optical conductivity and contributions from various physical processes of Fe_3O_4. The solid line is the optical conductivity of Fe_3O_4.

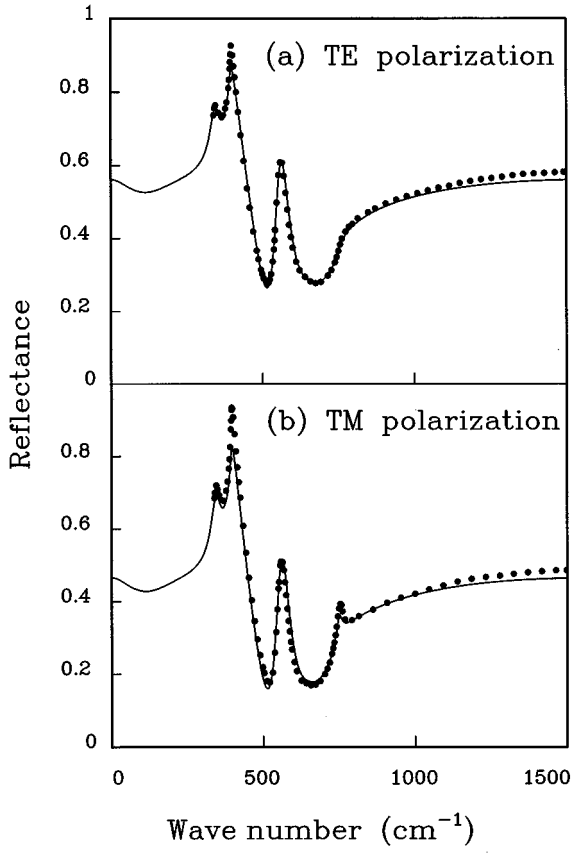

FIG. 2. Polarization-dependent experimental reflectances (solid circles) and theoretical ones (solid lines): (a) TE and (b) TM polarizations. Note that a peak structure can be seen near 756 cm^{-1} only in TM polarization.

the spectrum was taken with a relatively low resolution, i.e., 4 cm^{-1}, interference fringes due to the multiple reflections inside the substrate did not appear. Figure 1(a) shows two strong TO phonon peaks of Fe_3O_4 at 347 and 561 cm^{-1} and one TO peak of MgO at 398 cm^{-1}.[13,14] Note that an interesting peak structure appears at 756 cm^{-1}, which is close to one of LO phonon frequencies of bulk MgO, i.e., $\omega_{LO}^{MgO}=729$ cm^{-1}.[13]

To find the origin of the peak appearance, polarization dependence was investigated. The reflectance spectra measured with TE- and TM-polarized lights are shown as solid circles in Figs. 2(a) and 2(b), respectively. As shown in Fig. 2(a), in the case of TE polarization, no peak structure appears in the frequency region of our interest. Considering the configuration in TE polarization, it is clear that the $\vec{E}$-field component parallel to the film surface cannot induce the peak near 756 cm^{-1}. In the case of TM polarization, a clear peak structure does appear in the reflectance spectrum, as shown in Fig. 2(b). Therefore, the peak in Fig. 1(a) should come from the $\vec{E}$-field component normal to the film in TM polarization and be related to the longitudinal response of the Fe_3O_4/MgO film. Since only a longitudinal response located near the observed peak position is that of the MgO LO phonon, we can infer that the peaks shown in Figs. 1(a) and 2(b) are closely related to the MgO LO phonon at 729 cm^{-1}. As far as we know, it is the first time that a substrate LO phonon is observed in reflectance spectra of a film geometry.

To get further understanding on the newly observed phenomenon, the peak frequency, ω_{max}, of the MgO LOPR peak was measured with various values of θ_0. Figure 3 shows the angle dependence of TM reflectance. As θ_0 increases, ω_{max} moves toward a higher frequency and the peak becomes stronger. The measured values of ω_{max} are plotted in Fig. 4 with solid circles.

III. DATA ANALYSIS

To understand the observation of the MgO LOPR peak in the reflectance spectra, various computer simulations have been performed. In order to calculate the reflectance spectra of the Fe_3O_4 film on a MgO substrate, a three-phase model is used. As shown in Fig. 5, the light enters from vacuum with the incident angle θ_0. The thickness of the film is d and that of the substrate is assumed to be infinite. In Fig. 5, f, s, and 0 are used for subscripts to represent film, substrate, and vacuum, respectively. For calculations, the Fresnel coefficients for TE and TM polarizations are used and multiple reflections at the boundaries of the film are added coherently.[15]

To explain our experimental results on the Fe_3O_4/MgO film, the dielectric constants of MgO and Fe_3O_4 should be

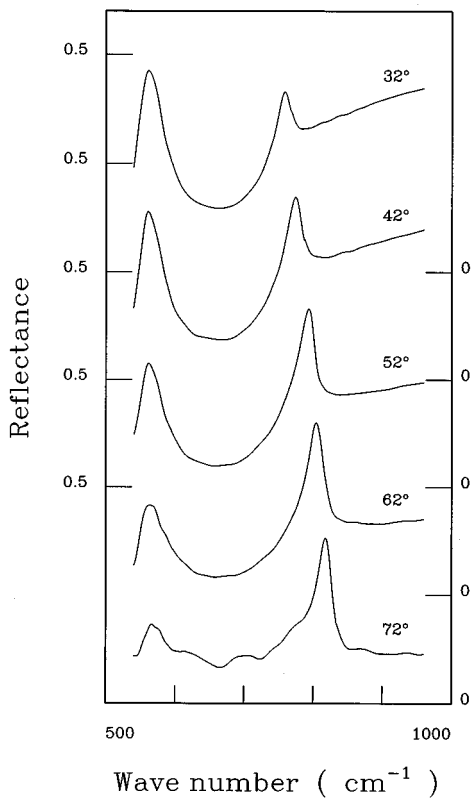

FIG. 3. TM reflectances measured on the Fe_3O_4/MgO film at various incident angles.

known. For the dielectric constant of MgO, $\tilde{\epsilon}_{\mathrm{MgO}}$, the Lorentz oscillator model is used:

$$\tilde{\epsilon}_s(\omega)=\tilde{\epsilon}_{\mathrm{MgO}}=\epsilon_\infty+\sum_{j=1}^{2}\frac{4\pi\rho_j\omega_j^2}{\omega_j^2-\omega^2-i\gamma_j\omega}, \qquad (1)$$

where ω_j, γ_j, and $4\pi\rho_j$ are the frequency, the damping constant, and the strength of jth TO phonon of MgO, respectively. Also, ϵ_∞ accounts for dielectric contributions from

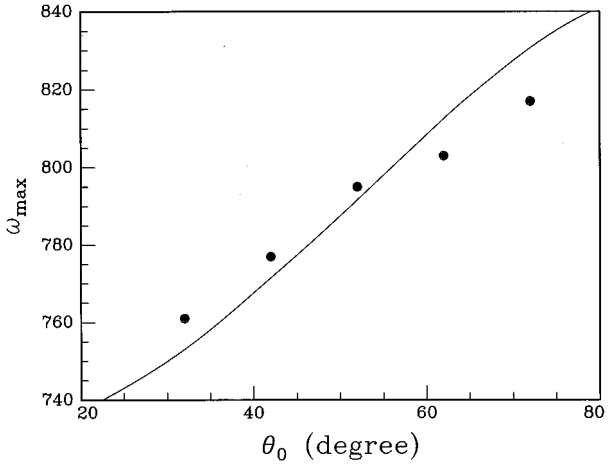

FIG. 4. The dependence of substrate LOPR peak frequency, $\omega_{\max}$, on the incident angle, θ_0. Solid circles show experimental peak positions obtained from Fig. 3. Solid line is derived from a resonance condition such as $\tilde{\epsilon}_s(\omega_{\max})=\sin^2\theta_0$.

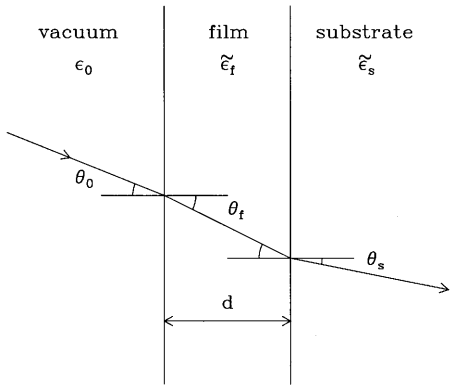

FIG. 5. Schematic diagram of the three-phase model.

interband transitions in the ultraviolet and soft x-ray regions. From the literature,[13] ϵ_∞ is estimated to be 3.01. It is well known that MgO has two TO phonon bands: $\omega_1=396$ cm^{-1}, $\gamma_1=7.60$ cm^{-1}, $4\pi\rho_1=6.80$, $\omega_2=643$ cm^{-1}, $\gamma_2=90$ cm^{-1}, and $4\pi\rho_2=0.043$.

Optical properties of Fe_3O_4 single crystal[14] and thin film[12] have been investigated. In both studies, it was found that the dielectric constant of Fe_3O_4, $\tilde{\epsilon}_{\mathrm{Fe_3O_4}}$, in the infrared region could be explained using a small polaron hopping model of Ihle *et al.*,[16]

$$\tilde{\epsilon}_f(\omega)=\tilde{\epsilon}_{\mathrm{Fe_3O_4}}=\tilde{\epsilon}_{\mathrm{Drude}}+\tilde{\epsilon}_{\mathrm{phonon}}+\tilde{\epsilon}_{d\text{-}s}+\tilde{\epsilon}_{\mathrm{hopping}}, \qquad (2)$$

where $\tilde{\epsilon}_{\mathrm{Drude}}$, $\tilde{\epsilon}_{\mathrm{phonon}}$, $\tilde{\epsilon}_{d\text{-}s}$, and $\tilde{\epsilon}_{\mathrm{hopping}}$ denote contributions of Drude-type free carriers, phonons, *d-s* interband transition, and small polaron hopping process of Fe_3O_4, respectively. The optical conductivity, $\tilde{\sigma}_{\mathrm{Fe_3O_4}}(\omega)$, can be evaluated using $\tilde{\sigma}_{\mathrm{Fe_3O_4}}(\omega)=-i(\omega/4\pi)\tilde{\epsilon}_{\mathrm{Fe_3O_4}}(\omega)$. The real part of the optical conductivity, σ_1, for Fe_3O_4 used in our calculation is shown in Fig. 1(b) as a solid line. Contributions of the Drude-type free carriers, phonons, *d-s* interband transition, and small polaron to $\sigma_1(\omega)$ are shown with dotted, dashed, dash-dotted, and dash–double-dotted lines, respectively.[14] Note that σ_1 of Fe_3O_4 is very large in the mid-infrared region due to the polaron hopping process and the *d-s* interband transition.

With $\tilde{\epsilon}_{\mathrm{MgO}}$ and $\tilde{\epsilon}_{\mathrm{Fe_3O_4}}$, given in Eqs. (1) and (2), reflectance spectra were calculated within the three-phase model. The theoretical spectra for TE and TM polarizations are shown in Fig. 2 as solid lines. For the case of unpolarized light, a spectrum is obtained by averaging the spectra of TE and TM polarizations and the result is shown in Fig. 1(a) as a solid line. The theoretical spectra in Figs. 1(a) and 2 are in good agreement with the experimental spectra. The agreements between the theoretical and experimental reflectance spectra suggest that the appearance of the substrate LOPR peak is contained in the Fresnel formula and can be explained by the three-phase model. However, the physical origin of the LOPR peak is difficult to be understood since the Fresnel formula are highly nonlinear and complicated equations.

IV. DISCUSSION

To get further understandings on the appearance of the MgO LOPR peak, some more computer simulations were performed for various simple cases. First, it is important to check whether the MgO LOPR peak is able to be seen without any film layer. TM reflectances of a single crystal MgO were evaluated with various angle of incidence. The calculated reflectance always showed a minimum (i.e., a dip instead of a peak) near ω_{LO}^{MgO}. Therefore, it is clear that the bulk MgO spectra themselves cannot explain the LOPR peak structure in the Fe_3O_4/MgO film, shown in Figs. 1(a) and 2(b).

A. Reflectance spectra of a simple Drude metal film on a MgO substrate

Since the dielectric constant of Fe_3O_4, given by Eq. (2), is complicated, it is rather difficult to understand the physical origin of the LOPR peak appearance. It would be useful to study behaviors of a metal film whose dielectric constant can be written in a simpler form. Therefore, reflectance spectra of a film which is composed of a simple Drude metal, such as gold, on a MgO substrate are calculated. The dielectric constant of the film is assumed to be

$$\tilde{\epsilon}_f = \epsilon_\infty + i\frac{4\pi\sigma_D}{\omega(1-i\omega\tau)}, \tag{3}$$

where σ_D and τ are dc conductivity and relaxation time of the metal, respectively. With Drude parameters for gold ($\epsilon_\infty = 1$, $\sigma_D = 4.9\times10^5\ \Omega^{-1}\ \mathrm{cm}^{-1}$, and $\tau = 3.0\times10^{-14}$ s),[17] the reflectance spectra for TM-polarized light entering with $\theta_0 = 30^o$ are calculated. Figure 6 shows reflectance spectra for the Drude-type metal film with various thicknesses ranging from 0 to 100 Å. The bottom curve shows the reflectance of the bulk MgO, which has a falling edge of the Reststrahlen band near ω_{LO}^{MgO}. When a very thin metal film is present (e.g., 5 Å), a dip structure is formed near the same frequency. However, as the film thickness increases, the reflectance level increases and the dip structure becomes weaker due to the screening of free carriers.

Disappearance of the substrate phonon structure in the reflectance spectra of the films thicker than 100 Å can be understood roughly in terms of skin depth, δ. The intensity of the $\vec{E}$ field inside a metal decreases exponentially. The characteristic length, δ, for the exponential decay of this $\vec{E}$ field can be written as:[18]

$$\delta = \frac{c}{\omega\sqrt{[(\epsilon_1^2+\epsilon_2^2)^{1/2}-\epsilon_1]/2}}, \tag{4}$$

where c is the speed of light. The skin depth of gold is about 200 Å near ω_{LO}^{MgO}, so the light cannot probe the substrate effectively for films thicker than 100 Å.

It is quite interesting that, for the simple Drude metal film, the dip structure appears instead of the observed LOPR peak structure of the Fe_3O_4 film. Since the scattering rate, $1/\tau$, of free carriers of gold is about 180 cm^{-1}, which is smaller than ω_{LO}^{MgO}, the frequency region where the MgO LO phonon locates corresponds to the relaxation skin effect region (i.e., $\omega\tau > 1$).[19,20] In this frequency region, the $\vec{E}$ field of light wave oscillates many times between collisions of the carriers. Due to the inertia of the carriers, the induced current lags behind the field by an increasing amount as the light frequency increases. So, the phase lag approaches 90^o, and light absorption becomes negligible. In this limit, the bulk metal sample should show very high reflectance due to the strong screening effect of the free carriers.[19] On the other hand, the metal film whose thickness is smaller than the skin depth might reveal the minimum of the substrate reflectance near ω_{LO}^{MgO}, resulting in the dip structure, shown in Fig. 6. The relaxation behaviors are characteristics of most of the other good metals, such as Ag and Cu, in the infrared region, so the substrate LOPR peak cannot be observed with such metal films.

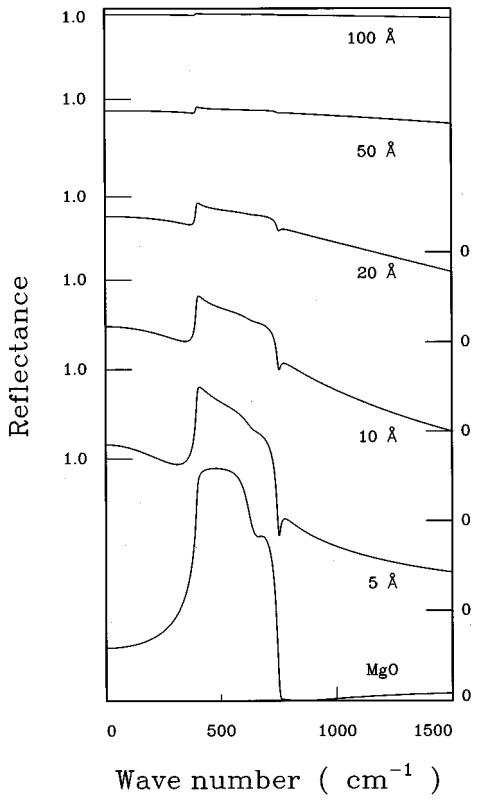

FIG. 6. TM reflectances calculated for a gold film with various thicknesses.

Note that the infrared conductivity of Fe_3O_4, shown in Fig. 1(b), is quite different from that predicted by the Drude model in the relaxation skin effect region. Contrary to predictions of the Drude model for good metals, the infrared conductivity of Fe_3O_4 near ω_{LO}^{MgO} remains almost as large as the DC conductivity. Even though the contributions to σ_1 for Fe_3O_4 might come from several mechanisms,[14] its nearly constant conductivity near ω_{LO}^{MgO} can be modeled *approximately* by the Drude model in the classical skin effect region ($\omega\tau < 1$):[19,20]

$$\tilde{\epsilon}_f \simeq \epsilon_\infty - 4\pi\sigma_D\tau + i\frac{4\pi\sigma_D}{\omega}. \tag{5}$$

In this frequency region, mean free path of the carrier is sufficiently small and frequency of the light wave is so low

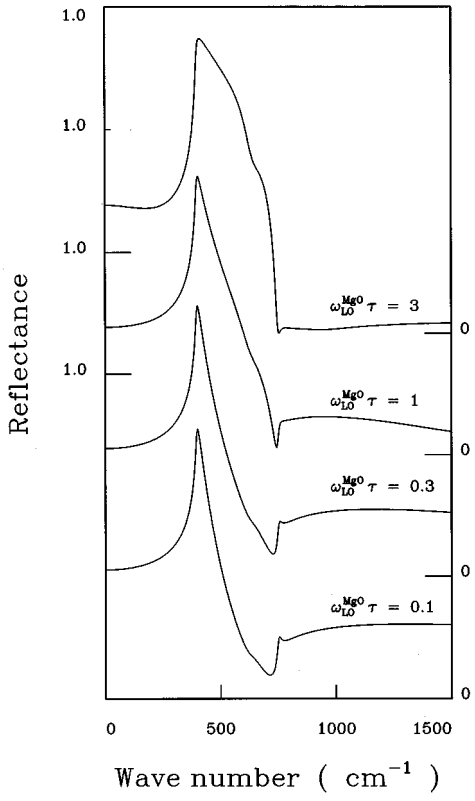

FIG. 7. TM reflectances calculated for a metal film with various values of $1/\tau$. $\sigma_D = 170\ \Omega^{-1}\ \mathrm{cm}^{-1}$, $\epsilon_\infty = 3$, and $d = 3000$ Å are assumed.

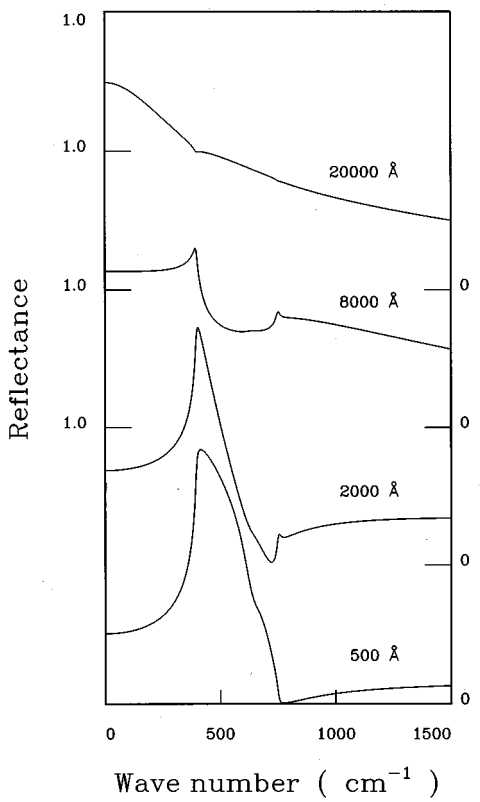

FIG. 8. TM reflectances calculated for a metal film with various thicknesses. The metal film is assumed to be in a frequency region of the classical skin effect ($\omega_{LO}^{MgO}\tau = 0.1$). The conductivity of film and the incident angle is fixed to be $170\ \Omega^{-1}\mathrm{cm}^{-1}$ and 30°, respectively.

that the carrier suffers many collisions during one period of light wave. Then, the optical conductivity should be almost independent of the frequency. The induced current is in phase of the wave, so there is a strong absorption of light.[19]

To clarify the role of carrier dynamics near ω_{LO}^{MgO}, computer simulations were performed for metallic films with various values of $1/\tau$. $\sigma_D = 170\ \Omega^{-1}\ \mathrm{cm}^{-1}$, $\epsilon_\infty = 3$, and $d = 3000$ Å are assumed. As shown in Fig. 7, in the relaxation skin effect region ($\omega\tau > 1$), a dip structure related to the reflectance of MgO can be seen. On the other hand, in the classical skin effect region ($\omega\tau < 1$), a peak structure can be seen near ω_{LO}^{MgO}. This figure suggests that the infrared absorption, related to the carrier dynamics, plays quite an important role on the appearance of LOPR peak in a metallic film.

The magnitude of infrared conductivity plays two roles on the appearance of substrate LOPR peak. When it is small, there is little light absorption and substrate LOPR cannot be seen. However, when it is too large, the skin depth becomes small so light cannot probe the substrate LO phonon when the film thickness is larger than δ. The role of the skin depth effect is shown in Fig. 8, where the reflectance spectra of metal films with various thicknesses are displayed. The dielectric constant of the metal film is again approximated by the Drude model in the classical skin effect region: $\omega_{LO}^{MgO}\tau = 0.1$ and $\sigma_D = 170\ \Omega^{-1}\ \mathrm{cm}^{-1}$. It can be seen that the substrate LOPR peaks are able to appear in the film whose thickness is roughly less than the skin depth ($\delta = 8900$ Å for this case).

B. A simple model for the substrate LOPR peak

Our experiments and computer simulations show that there are three requirements for the substrate LOPR to appear in reflectance spectra of a metallic film. First, the incoming light should have the $\vec{E}$-field component perpendicular to the film; namely, it should have TM polarization. Second, the carriers in a metallic film layer should absorb the light strongly: for a Drude-type metal, the LO phonon should be located at a frequency which belongs to the classical skin effect region. Third, the thickness of the film should be smaller than the skin depth.

From these constraints, a simple but qualitatively physical model can be proposed. When a TM-polarized light enters a metallic film with an oblique angle, the $\vec{E}$-field component normal to the film surface will induce an oscillating current along the same direction. Then, the charge oscillation inside the metal can be coupled to the LO phonon of a substrate. Therefore, the LOPR peak structure can appear near the substrate LO phonon frequency.

Our simple model also provides explanations on the dependence of ω_{max} on θ_0, which is shown in Fig. 4. For TM-polarized light, the $\vec{H}$ field is parallel to the film boundaries. From the boundary conditions for $\vec{H}$ and $\vec{E}$ fields, the normal and tangential components of the $\vec{E}$ field at the interface between film and substrate can be derived:[21]

$$E_n = -\sin\theta_0 \sqrt{\frac{\mu_0}{\epsilon_0}} \frac{H}{\tilde{\epsilon}_f} \quad \text{on film side,} \tag{6}$$

$$E_n = -\sin\theta_0 \sqrt{\frac{\mu_0}{\epsilon_0}} \frac{H}{\tilde{\epsilon}_s} \quad \text{on substrate side,} \tag{7}$$

and

$$E_t = \sqrt{\tilde{\epsilon}_s - \sin^2\theta_0} \sqrt{\frac{\mu_0}{\epsilon_0}} \frac{H}{\tilde{\epsilon}_s} \quad \text{on both sides,} \tag{8}$$

where H represents the intensity of the $\vec{H}$ field at the boundary. When $\tilde{\epsilon}_s$ equals $\sin^2\theta_0$, the $\vec{E}$ field has only a normal component E_n because the tangential component E_t vanishes. In other words, when a resonance condition, $\tilde{\epsilon}_s = \sin^2\theta_0$, is valid, the $\vec{E}$ field is perpendicular to the interface and induces current in the Fe_3O_4 film along the longitudinal direction effectively. And, such a longitudinal oscillation of free carriers in the film will be able to be coupled to the LO phonon mode of a substrate. Therefore, the substrate LOPR peak becomes the strongest at a frequency where the resonance condition is satisfied:

$$\tilde{\epsilon}_s(\omega_{\max}) \simeq \sin^2\theta_0 . \tag{9}$$

This equation is similar to the well-known expression for a critical angle of total internal reflection, except that the incident angle θ_0 is involved. In Fig. 4, the frequency values, which satisfy Eq. (9) for the MgO substrate, are shown as a solid line. (Measured values of the dielectric constant of MgO in Ref. 13 were used in actual calculation.) As shown in this figure, the resonance condition, shown in Eq. (9), can explain the incident angle dependence of $\omega_{\max}$ reasonably well. More studies are required to understand this new phenomenon quantitatively.

It is important to compare our result with the Berreman effect. In the latter case, the reflectance spectra of a film show a dip at a *film* LO phonon frequency due to polarization charges induced on the film boundaries. The polarization charges are directly coupled with the *film* LO phonon, providing an infrared absorption. In our study, the incident light induces a current in a metallic film, which can be coupled to the *substrate* LO phonon. So, it provides a new way of probing a LO phonon of a bulk material.

The Berreman effect has been applied by many workers for characterizing the LO phonons of films themselves. It is required to get high quality films in order to use the Berreman effect, but it is usually difficult to get such high quality films. On the other hand, our work demonstrates that LO phonon of a solid can be probed by infrared spectroscopy by depositing a metallic film with strong infrared absorption.[22] Compared to the case of the Berreman effect, quality of the film does not have to be so high that this method can be more easily applied for various solids.

V. SUMMARY

Infrared reflectance spectra were measured on a Fe_3O_4 film deposited on a bulk MgO substrate. For an obliquely incoming light with TM polarization, a peak structure was detected near $\omega_{\rm LO}$ of MgO. To understand the physical origin of the MgO LOPR peak in the reflectance spectra, various computer simulations have been performed within the three-phase model. From our experiments and simulations, some constraints are found for the substrate LOPR to appear: (i) TM-polarized light, (ii) strong absorption in a metallic film layer around $\omega_{\rm LO}$ of a substrate, and (iii) film thickness smaller than the skin depth. A simple but qualitatively physical model could be constructed; when a TM-polarized light enters a metallic film with an oblique angle, the $\vec{E}$-field component normal to the film surface will induce an oscillating current along the same direction. Then, the charge oscillation inside the metal can be coupled to the LO phonon of a substrate. Therefore, the LOPR peak structure can appear at the substrate LO phonon frequency. Our simple model also provides explanations on the resonance condition, such as $\tilde{\epsilon}_s(\omega_{\max}) \simeq \sin^2\theta_0$. This newly observed phenomenon might be useful to optically investigate a LO phonon of a solid, where other methods are difficult to be applied.

ACKNOWLEDGMENTS

We would like to appreciate the ICNSRF for allowing us to use their facilities. This work was supported by the Ministry of Education through the Basic Science Research Institute program BSRI-95-2416 and by the Korea Science and Engineering Foundation (KOSEF) through the RCDAMP at Pusan National University.

*Electronic address: jsahn@phya.snu.ac.kr
†Electronic address: twnoh@phya.snu.ac.kr

[1] C. Kittel, *Introduction to Solid State Physics* (Wiley, New York, 1986), pp. 271–278.
[2] P. Brüesch, *Phonons: Theory and Experiments I*, Springer Series in Solid-State Sciences Vol. 65 (Springer-Verlag, Berlin, 1982).
[3] R. E. Peierls, *Quantum Theory of Solids* (Clarendon, Oxford, 1956), pp. 54–58.
[4] For anisotropic bulk crystals, longitudinal phonon mode features have been found. For example, see A. S. Barker and M. Ilegems, Phys. Rev. B **7**, 743 (1973); J. L. Duarte, J. A. Sanjurjo, and R. S. Katiyar, *ibid.* **36**, 3368 (1987).
[5] D. W. Berreman, Phys. Rev. **130**, 2193 (1963).
[6] O. E. Piro, Phys. Rev. B **36**, 3427 (1987).
[7] Z. Schlesinger, L. H. Greene, and A. J. Sievers, Phys. Rev. B **32**, 2721 (1985).
[8] K. Hübner, L. Schumann, A. Lehmann, H. H. Vajen, and G. Zuther, Phys. Status Solidi B **104**, K1 (1981).
[9] O. E. Piro, S. R. González, and P. J. Aymonino, Phys. Rev. B **36**, 3125 (1987).
[10] O. Hunderi, Physica A **157**, 309 (1987).
[11] F. Fuchs, J. Schmitz, K. Schwarz, J. Wagner, J. D. Ralston, P. Koidl, C. Gadaleta, and G. Scamarcio, Appl. Phys. Lett. **65**, 2060 (1994).
[12] H. S. Choi, J. S. Ahn, W. Jo, and T. W. Noh, J. Korean Phys. Soc. **28**, 636 (1995).
[13] D. M. Roessler and D. R. Huffman, in *Handbook of Optical Constants of Solids II*, edited by E. D. Palik (Academic, San Diego, 1991), pp. 919–955.
[14] For detailed analytical expressions of $\tilde{\epsilon}_{Fe_3O_4}$ in the small polaron model, refer to L. Degiorgi, P. Wachter, and D. Ihle, Phys. Rev. B **35**, 9259 (1987).

[15] M. Born and E. Wolf, *Principles of Optics* (Pergamon, Oxford, 1980), pp. 36–70.
[16] D. Ihle and B. Lorenz, J. Phys. C: Solid State Phys. **18**, L647 (1985); **19**, 5239 (1986).
[17] N. W. Ashcroft and N. D. Mermin, *Solid State Physics* (Saunders College, New York, 1976), pp. 8–10.
[18] J. D. Jackson, *Classical Electrodynamics* (Wiley, New York, 1975), pp. 296–298.
[19] F. Wooten, *Optical Properties of Solids* (Academic, New York, 1972), pp. 90–94.
[20] J. M. Ziman, *Principles of the Theory of Solids* (Cambridge University Press, London, 1972), pp. 278–282.
[21] B. Harbecke, B. Heinz, and P. Grosse, Appl. Opt. A **38**, 263 (1985).
[22] Various metallic oxide films, including high T_c superconductors, are known to have strong infrared absorption. For high T_C materials, refer to T. Timusk and D. B. Tanner, in *Physical Properties of High Temperature Superconductors I*, edited by D. M. Ginsberg (World Scientific, Singapore, 1989), pp. 339–407.